



HAL
open science

Set1-dependent H3K4 methylation becomes critical for limiting DNA damage in response to changes in S-phase dynamics in *Saccharomyces cerevisiae*

Christophe de La Roche Saint-André, Vincent Géli

► To cite this version:

Christophe de La Roche Saint-André, Vincent Géli. Set1-dependent H3K4 methylation becomes critical for limiting DNA damage in response to changes in S-phase dynamics in *Saccharomyces cerevisiae*. *DNA Repair*, 2021, 105, pp.103159. 10.1016/j.dnarep.2021.103159 . hal-03431382

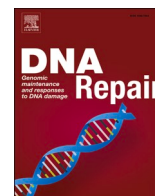
HAL Id: hal-03431382

<https://hal.science/hal-03431382>

Submitted on 25 Nov 2021

HAL is a multi-disciplinary open access archive for the deposit and dissemination of scientific research documents, whether they are published or not. The documents may come from teaching and research institutions in France or abroad, or from public or private research centers.

L'archive ouverte pluridisciplinaire **HAL**, est destinée au dépôt et à la diffusion de documents scientifiques de niveau recherche, publiés ou non, émanant des établissements d'enseignement et de recherche français ou étrangers, des laboratoires publics ou privés.



Set1-dependent H3K4 methylation becomes critical for limiting DNA damage in response to changes in S-phase dynamics in *Saccharomyces cerevisiae*

Christophe de La Roche Saint-André^{1,*}, Vincent Géli¹

Marseille Cancer Research Center (CRCM), U1068 Inserm, UMR7258 CNRS, Aix Marseille University, Institut Paoli-Calmettes, Marseille, France

ARTICLE INFO

Keywords:

Set1
H3K4 methylation
Replication stress
DNA damage

ABSTRACT

DNA replication is a highly regulated process that occurs in the context of chromatin structure and is sensitive to several histone post-translational modifications. In *Saccharomyces cerevisiae*, the histone methylase Set1 is responsible for the transcription-dependent deposition of H3K4 methylation (H3K4me) throughout the genome. Here we show that a combination of a hypomorphic replication mutation (*orc5-1*) with the absence of Set1 (*set1Δ*) compromises the progression through S-phase, and this is associated with a large increase in DNA damage. The ensuing DNA damage checkpoint activation, in addition to that of the spindle assembly checkpoint, restricts the growth of *orc5-1 set1Δ*. The opposite effects of the lack of RNase H activity and the reduction of histone levels on *orc5-1 set1Δ* viability are in agreement with their expected effects on replication fork progression. We propose that the role of H3K4 methylation during DNA replication becomes critical when the replication forks acceleration due to decreased origin firing in the *orc5-1* background increases the risk for transcription replication conflicts. Furthermore, we show that an increase of reactive oxygen species levels, likely a consequence of the elevated DNA damage, is partly responsible for the lethality in *orc5-1 set1Δ*.

1. Introduction

Replication of chromosomal DNA is central for faithful genome propagation across cell divisions. It initiates at discrete genomic loci called origins of replication that are distributed along chromosomes [1]. The origins of replication in *Saccharomyces cerevisiae* are defined by short DNA sequences called autonomous replicating sequences (ARS) that are the sites of the cell cycle regulated assembly of prereplicative complexes (pre-RCs). The origin recognition complex (ORC) binds to ARS and, together with Cdc6 and Cdt1, is required for the loading of the Mcm2-7 complex, the replicative DNA helicase, during the G1-phase of the cell cycle. S-phase entry involves activation of the pre-RCs through phosphorylation of Mcm2-7 and recruitment of additional factors, converting the pre-RC into a pair of diverging replisomes [1]. The progression of the replication fork relies on the activated form of the helicase known as Cdc45/Mcm2-7/GINS complex, which unwinds the

DNA, followed by the DNA polymerases that carry out the synthesis of DNA at the leading and lagging strands [1].

Among the various obstacles that can be encountered by replication forks during their progression, those linked to transcription are potentially a major challenge [2]. Transcription-replication conflicts (TRCs) are prominent when the transcription machinery and the replisome are converging (head-on orientation). TRCs can result from the presence of either the transcription machinery itself or some transcription-induced/stabilized non-B DNA structures, such as R-loops which consist of DNA-RNA hybrids together with displaced single-stranded DNA (ssDNA) [2]. If sufficiently stable, R-loops can lead to the stalling of forks which, due to polymerase/helicase uncoupling and/or nucleolytic resection, are also a source of ssDNA [3]. The ssDNA of R-loops and stalled forks is rapidly coated by the ssDNA binding protein RPA [4,5]. The accumulation of RPA-coated ssDNA provides the signal for the recruitment of the Mec1/ATR checkpoint kinase to the

Abbreviations: ARS, autonomous replicating sequences; pre-RCs, prereplicative complexes; ORC, origin recognition complex; TRCs, transcription-replication conflicts; ssDNA, single-stranded DNA; DSBs, double-strand breaks; HR, homologous recombination; HU, hydroxyurea; SAC, spindle assembly checkpoint; ROS, reactive oxygen species.

* Corresponding author.

E-mail address: christophe.laroche@inserm.fr (C. de La Roche Saint-André).

¹ Equipe labellisée par la Ligue Nationale Contre le Cancer.

<https://doi.org/10.1016/j.dnarep.2021.103159>

Received 10 February 2021; Received in revised form 27 May 2021; Accepted 13 June 2021

Available online 18 June 2021

1568-7864/© 2021 The Author(s).

Published by Elsevier B.V. This is an open access article under the CC BY-NC-ND license

(<http://creativecommons.org/licenses/by-nc-nd/4.0/>).

defective replication fork [6,7]. The activation of Mec1 which results from this interaction can block mitosis in response to replication defects [8]. The processing of R-loops and stalled forks, that may eventually collapse, lead to the formation of double-strand breaks (DSBs). In this case, the repair of DSBs and therefore the possible restart of the fork depends on Rad52-dependent homologous recombination (HR) to repair the broken DNA [9,10].

Some functional links between H3K4 methylation and replication have been described. In yeast, plants and mammalian cells, H3K4me2 and H3K4me3 are enriched on replication origins [11–13]. In human cells, the near-universal presence of dimethylated H3K4 at ORC2 sites led to consider it as a candidate mark recognized by ORC [14], and H3K4me3 demethylation was shown to promote replication origin activation by driving the chromatin binding of Cdc45 [15]. Additional work provided evidence that the MLL complexes and methylated H3K4 are involved in DNA replication through the replication licensing process [16]. Altogether, these studies point to a role of H3K4 methylation in DNA replication at the level of origin function. In *Saccharomyces cerevisiae*, the Set1-dependent H3K4 dimethylation has been described to promote replication origin function [11]. This would partly explain why *set1Δ* cells display a delayed entry into S-phase in mitotic cells [17], as well as meiotic cells [18], although in mitotic cells this delay was proposed to be caused by Set1 contribution to proper cell-cycle-dependent gene expression [17]. Furthermore, Set1-dependent H3K4 dimethylation requirement for efficient origin activation [11] was not supported by an independent study where the recruitment and activation of DNA replication initiation factors was unaffected by the loss of H2B ubiquitylation [19], a context in which H3K4 dimethylation is absent [20]. Such discrepancy could be related to the fact that distinct replication origins were analyzed with alternative experimental methods. However, it is also possible that H3K4 methylation could influence DNA replication independently of origin firing as in the case of H2B ubiquitylation [19]. Recent works described the involvement of Set1 in DNA replication beyond origin firing. First, Set1 is important for the completion of DNA replication after an acute exposure to hydroxyurea (HU) [21]. The slower recovery of *set1Δ* from HU exposure is not the consequence of a defect in origin initiation but most likely in the processing of HU-stalled forks. Second, Set1 has a role in protecting the genome from TRCs occurrence with the transcription-deposited H3K4 methylation decelerating the fork progression at highly transcribed regions [22].

We have reinvestigated the conjecture that the genetic interactions that exist between *set1Δ* and replication-initiation mutants are related to origin firing defects [11]. We found that, when associated to the *orc5-1* mutation, that affect the subunit 5 of the ORC complex, the loss of Set1 leads to a strong defect of S-phase progression in mitotic and in meiotic cells. We failed to correlate this to a defect in origin function in *orc5-1 set1Δ* and instead we observed a strong increase in both the number and intensity of nuclear RPA and Rad52 foci, a sign of DNA damage accumulation in the double mutant. Accordingly, the DNA damage checkpoint acts together with the spindle assembly checkpoint to restrict the growth of *orc5-1 set1Δ* cells. Because *orc5-1 set1Δ* viability is decreased by the lack of RNase H activity but rescued by the reduction of histone gene dosage, we propose that the role Set1 plays in TRCs mitigation [22] becomes critical when replication fork velocity is increased due to the *orc5-1* mutation. On another hand, *orc5-1 set1Δ* cell death is partly the consequence of reactive oxygen species (ROS) accumulation, likely in response to DNA damage.

2. Materials and methods

2.1. Yeast strains and growth conditions

All strains used in this study are in the W303 or SK1 background and are listed in S1 Table. Standard conditions were used to grow and maintain strains on YPD (yeast extract-peptone-dextrose). Construction

of *de novo* gene deletion strains was performed by PCR-mediated recombination and all double-mutant construction was performed by mating. For genetic complementation assays in *orc5-1 set1Δ* (Fig. 1A, middle), wild-type Set1 and mutant Set1G951S proteins fused to the Gal DNA binding domain were expressed under the control of the *ADHI* promoter from constructs integrated at the *trp1-1* locus as previously described [23]. To generate rho^o strains, cells were grown to saturation in liquid YPD medium plus ethidium bromide (25 μg/mL) and plated on YPD plates for individual colonies. Clones were checked for growth defects on a nonfermentable carbon source (YPG 2% glycerol).

To analyse meiotic S-phase, after growth in rich glucose medium (YPD), exponential phase cells were pregrown in rich acetate medium (YPA; 1% potassium acetate, 2% bacto-peptone, 1% bacto yeast extract supplemented with 25% amino acids) during 8 h, then diluted at 2×10^6 cells/mL and grown in YPA during 14 h. Cells were washed once with water and then inoculated into sporulation medium (1% potassium acetate supplemented with 25% amino acids) and incubated at 30° with vigorous agitation. For measure of sporulation levels, cells were directly streaked from YPD plates on sporulation medium plates (1% potassium acetate supplemented with 25% amino acids). Sporulation rate was determined by counting asci visualized by light microscopy.

2.2. Spore colony growth analysis

Tetrad dissection was performed on YPD plates using the MSM 400 dissection microscope (Singer Instrument Company) and isolated spores were incubated three days at 25° or two days at 30°. JPEG files of dissection plates were analyzed with ImageJ [24] to measure the area of each spore-derived colony.

2.3. Temperature and DNA damage sensitivity assays

Freshly grown cells were taken, resuspended in water to 0.5 at OD₆₀₀, and ten-fold serially diluted. Seven microliters of yeast cells at different dilutions were then spotted on YPD media or on YPD media containing either various concentrations of HU, NaCl (1 M) or N-acetylcysteine (30 mM). Images were taken after incubation at the indicated temperatures for 2–5 days.

2.4. Plasmid maintenance assays

Plasmid maintenance assays were performed as described previously [11]. Yeast strains containing a *CEN4/ARS1/URA3* plasmid (pRM102, [25]) were grown to log phase in selective medium (lacking uracil) and 100–200 cells were plated on both selective and nonselective media to establish an initial percentage of plasmid-bearing cells. These cultures were also diluted to a concentration of 1×10^5 cells/mL in 5 mL of nonselective media and grown for 8–10 generations before once again plating on both selective and nonselective media. Precise generation numbers were calculated using the following formula: $n = \log(C_F/C_I)/\log(2)$, where C_F represents the final number of cells as measured by OD₆₀₀ and C_I represents the starting cell number of 10^5 cells/mL. After 2 days of growth, colonies were counted, and the plasmid loss rate (L) per generation (n) was calculated using the following formula: $L = 1 - (\%F/\%I)^{1/n}$, where %F is the final percentage of cells that retained the plasmid and %I is the initial percentage of cells that contain the plasmid.

2.4.1. Measurement of cell-cycle progression

Yeast cultures were grown at 25° to an A₆₀₀ of 0.6–0.8 then incubated 3 h with α-factor (50 ng/mL), 2 h at 25° then 1 h at 37°. Cells were washed two times with distilled water and one time with fresh YPD medium and released into the first cell cycle in YPD. Cell samples (1 mL) were collected for each time point and were fixed in 70% ethanol. After rehydration in PBS, the samples were incubated at least 2 h with RNase A (1 mg/mL) at 37°. Cells were resuspended in 50 μg/mL propidium

iodide in PBS for at least 15 min at room temperature. After a wash in PBS, cells were resuspended in 5 µg/mL propidium iodide, sonicated briefly to remove cell clumps, and the DNA content was determined by FACS with a Becton Dickinson FACSCalibur. Number of budding cells was counted under light microscope at each time point for 200–300 cells.

2.5. Fluorescence microscopy

Cells expressing Rfa1 tagged with cyan fluorescent protein (CFP) or Rad52 tagged with yellow fluorescent protein (YFP) were grown in liquid YPD (+ adenine) medium to exponential phase at 30°, harvested, washed in PBS, and placed on a glass slide. Observations of cells were performed using a Nikon Eclipse Ti microscope with a 100x oil immersion objective. Cell images were captured with a Neo sCMOS Camera (Andor). Fluorophores were visualized using band-pass CFP (Rfa1-CFP) or YFP (YFP-Rad52) filter sets. For each field of view, a single DIC image and 11 CFP or YFP images at 0.3 µm intervals along the Z-axis were acquired. CFP and YFP foci were visualized and quantified using ImageJ software. For each strain, at least 200 cells were scored for Rfa1-CFP or Rad52-YFP foci. Mean fluorescence intensity within constant square regions placed in the nucleus outside the foci area was measured to get the average nuclear background fluorescence (N). Based on cellular morphology, cells were grouped into G₁ phase (unbudded), S (small-budded), G₂/M (medium to large-budded, undivided nucleus), M (large-budded, divided nucleus) and G₂/M arrested (dumbbell-shaped cells with one nucleus). Quantification of cell morphology was determined by analysis of at least 200 cells at each time point.

2.6. Measurement of ROS levels

After an overnight incubation at 25°, cells were inoculated (A₆₀₀ of 0.2) in fresh YPD medium (supplemented with adenine) and grown at 25° or 32° during seven hours, with or without NAC (30 mM). About 10⁷ cells were collected, centrifugated, resuspended in 100 µl Tris EDTA 50 mM pH7.5 with 0.1 µl CellROX® Green reagent (Life Technologies) and incubated during 30 min at the same temperature of 25° or 32°. Intracellular levels of reactive oxygen species (ROS) was assessed by measuring the mean fluorescence using flow cytometry with a Becton Dickinson FACSCalibur. Control autofluorescence signals were obtained by incubating cells in absence of CellROX® Green reagent. To quantify ROS levels taking cell size into account, the difference between the mean CellROX® Green-dependent fluorescence signal and the mean autofluorescence signal was divided by the mean forward scatter (FSC) signal.

3. Results

3.1. Cell proliferation and viability of *orc5-1* is promoted by *Set1*

We first confirmed, in the W303 background, the existence of negative genetic interactions between the *SET1* deletion and temperature-sensitive alleles of various replication factors involved in origin function and replication initiation [11]: *orc5-1* (Fig. 1), *cdc6-4*, *mcm2-1* and *cdc17-1* (Fig. S1).

We focused on the *orc5-1* mutation as the genetic interaction with *set1Δ* was evident at 25° (see below), knowing that even at 23° only a subset of origins are activated in *orc5-1* [26]. Meiotic tetrads from a heterozygous *set1Δ/SET1 orc5-1/ORC5* diploid were dissected and the isolated spore colonies were grown at 25°. The colonies corresponding to *orc5-1 set1Δ* spores grew much more slowly than those of each single mutant (Fig. 1A, left). This growth defect was exacerbated at 30° (Fig. 1B), and at 32° the viability of *orc5-1 set1Δ* was severely compromised (Fig. 1C).

To demonstrate that the slow growth phenotype of *orc5-1 set1Δ* was indeed caused by the lack of *SET1*, we performed a rescue experiment by

adding a wild-type copy of *SET1* on a different chromosome (Fig. 1A, middle). The complete restoration of the colony growth ruled out a possibility that *SET1* deletion might have disturbed expression of the adjacent *ORC6* gene thus causing an indirect effect. Notably, the *set1-G951S* allele encoding a catalytically dead version of Set1 was not able to rescue the growth of the double mutant, indicating that the Set1 histone methylase activity is required. Furthermore, the impact of *set1Δ* was recapitulated when the two copies of histone H3 bear the K4R (unmethylatable) mutation (Fig. 1A, right), confirming the importance of H3K4 methylation for robust growth of the *orc5-1* mutant.

The loss of the COMPASS complex subunit *Spp1* is associated with a specific decrease of H3K4me3 levels, without affecting mono- and dimethylation of H3K4 [27]. Compared to *set1Δ*, the negative impact of *spp1Δ* on the growth of *orc5-1* was moderate (Fig. 1B), indicating that H3K4 trimethylation is partly dispensable for the growth of *orc5-1*, in contrast to mono- or dimethylation. Alternatively, this difference could be related to the larger increase of H3K4 acetylation levels in *set1Δ* compared to *spp1Δ* [28]. H3K4 acetylation mainly occurs in the absence of H3K4 methylation and essentially depends upon Gcn5, the catalytic subunit of different histone acetyltransferase (HAT) complexes, which is involved in the regulation of origin firing [29]. We therefore tested the impact of impairing H3K4 acetylation, through *GCN5* inactivation, on the thermosensitivity of *orc5-1*. Whereas the loss of Gcn5 had no effect by itself on *orc5-1* growth at 32°, the combination of *set1Δ* with *gcn5Δ* strongly affected the growth of *orc5-1* even at 25° (Fig. 1C). Sgf29 is another component of the Gcn5-dependent HAT complexes that is involved in their recruitment to chromatin, through its interaction with H3K4me2/3 [30]. The negative effect of *set1Δ* on *orc5-1* growth at 32° was similar in the absence of Sgf29 (Fig. 1C). Altogether, these results suggest that it is the lack of H3K4 methylation rather than the concomitant increase of Gcn5-dependent H3K4 acetylation that is responsible for the negative effect of *set1Δ* on *orc5-1* growth.

3.2. The primary cause of the *orc5-1 set1Δ* genetic interaction is not related to a defect in origin activation

Since replication origin function is affected in *orc5-1* [26] and the involvement of H3K4 methylation in the same process has been described [11], an additive defect at the level of origin activity could be the basis of the *orc5-1 set1Δ* genetic interaction. The conclusion of [11] was based on a plasmid loss assay that measures the ability of cells to maintain a minichromosome bearing a single replication origin and a centromere. However, according to a recent genome wide analysis, no replication initiation defects were detected in *set1Δ*, with the bulk of early origins being as efficiently activated as in the wild-type [21]. This global analysis however does not exclude some variation in the activity of individual origins. In any case, whether that defective origin function was in fact responsible for the observed Set1-dependent genetic interactions has not been thoroughly investigated [11].

Therefore, we set out to employ the plasmid loss assay to test whether the *orc5-1 set1Δ* genetic interaction is a manifestation of a synergistic defect in origin function. At 30°, both the rate of plasmid loss that we have measured in the wild-type and its increase in *set1Δ* (Fig. 2) were in agreement with the previous work [11]. A similar increment was observed in *orc5-1 set1Δ* relative to *orc5-1*, while the latter had much higher rate of plasmid loss compared to wild type. Importantly, in the context of *orc5-1*, the increased rate of plasmid loss due to lack of Set1 appears marginal compared to the drastic drop in viability (Fig. 1C). To exclude the possibility that this limited increase in plasmid loss was due to the saturation of the assay, the temperature of 25° was used in order to limit inactivation of the *orc5-1* encoded protein (Fig. 2). Again, despite the milder rate of plasmid loss in *orc5-1*, no substantial increase was associated with the loss of Set1, contrasting with a strong genetic interaction observed for the growth rate (Fig. 1A). While we cannot exclude some contribution, the activation of origins is likely not a determining factor in the *orc5-1 set1Δ* genetic interaction.

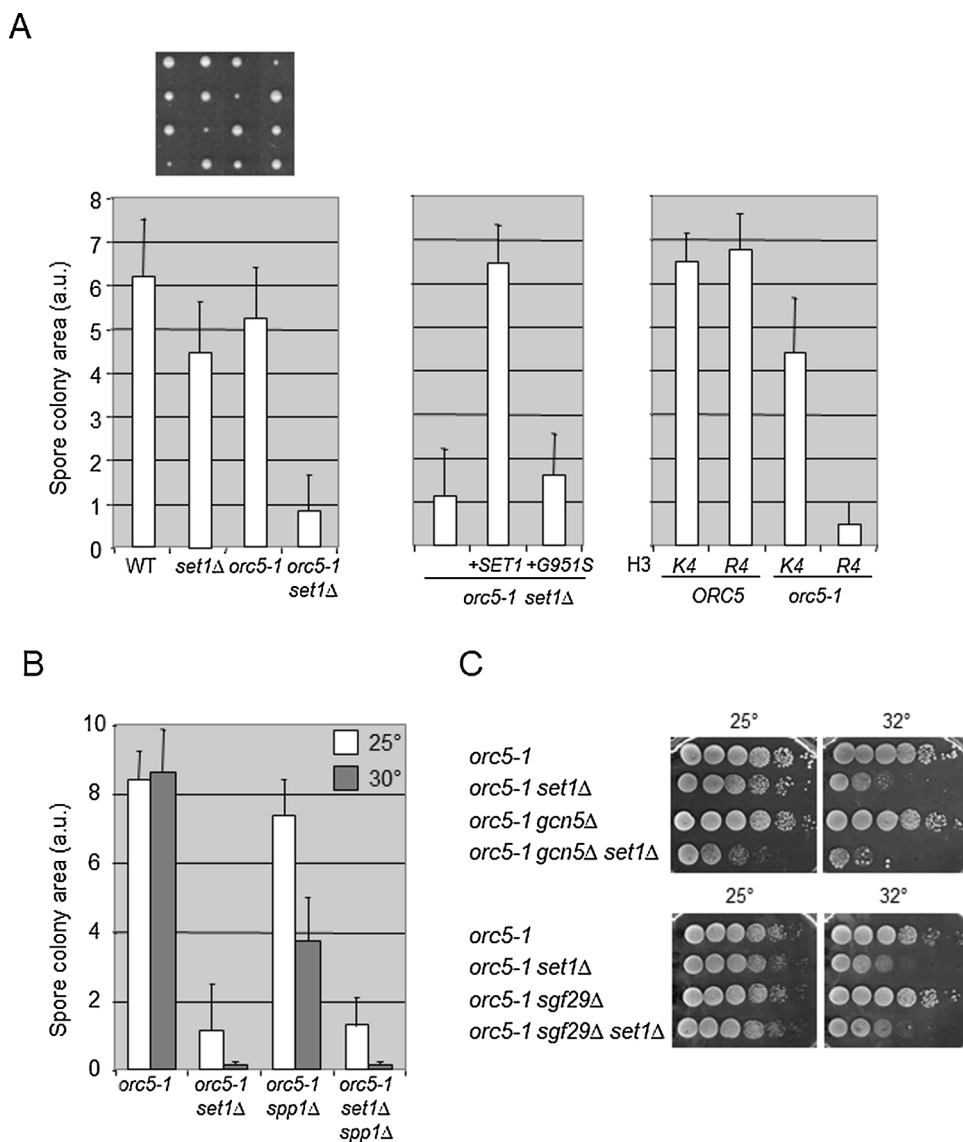


Fig. 1. Negative genetic interaction between *set1Δ* and *orc5-1*. A) Left: The deletion of *SET1* results in growth defect when combined with *orc5-1*. Growth of spore colonies after tetrad dissection of the diploid strain *set1Δ/SET1 orc5-1/ORC5*. The area of single-spore derived colonies was determined after three days at 25° since spore isolation (a.u.: arbitrary units). Error bars represent standard deviations of $n \geq 15$ spore colony area per genotype. Four representative tetrads (vertical lines), each with one small *orc5-1 set1Δ* colony, are shown on the top. Middle: Colony growth from *orc5-1 set1Δ* spores with an additional copy of *SET1* encoding either a wild-type (+*SET1*) or a catalytically inactive (+*G951S*) Set1 protein. Right: Colony growth from *ORC5* and *orc5-1* spores with wild-type copies (*K4*) and *K4R*-mutated copies (*R4*) of the H3 encoding genes *HHT1* and *HHT2*. B) Effect of *SPP1* deletion is minimal compared to that of *SET1*. Growth of spore colonies, at 25° and 30°, after tetrad dissection of the diploid strain *set1Δ/SET1 spp1Δ/SPP1 orc5-1/ORC5*. C) Thermosensitivity of *orc5-1 set1Δ* is independent of H3K4 acetylation. Tenfold serial dilutions of the respective strains were spotted onto YPD plates and incubated at the indicated temperatures for 3-4 days.

3.3. Progression through S-phase is compromised in *orc5-1 set1Δ* cells

Analysis of the cell cycle profiles by flow cytometry did not reveal any significant changes in the distribution along the cell cycle in *orc5-1 set1Δ* during exponential growth at 25°, excepted a relative increase of cells in G2/M phase (see -3 h on Fig. 3A). Cells were then arrested in late G1-phase by α -factor treatment during two hours, shifted to 37° for an additional hour to inactivate *orc5-1*, and then released from the G1 block at 37° (Fig. 3A). No delay in the progression through S-phase was apparent for *orc5-1* cells that completed DNA replication after 30 min, similarly to the wild-type. This suggests that any decrease in origin firing, as evidenced by the plasmid loss assay (Fig. 2), is compensated by an increase of the replication fork rate as shown previously for other mutations affecting the level of origin firing [31]. While *set1Δ* cells display a slight replication delay at 37°, the progression through S-phase was notably slower in *orc5-1 set1Δ* with most of the cells having less than 2C DNA content when replication is complete in both single mutants. Importantly, the entry into S-phase in *orc5-1 set1Δ*, as measured by the budding index, was similar to that of *set1Δ* and *orc5-1* (Fig. S2A). Therefore, Set1 loss appeared to affect S-phase progression when ORC function is compromised.

A progressive accumulation of cells with a 2C DNA content, suggesting a delay/arrest in G2/M, has been described for *orc5-1* cultures at

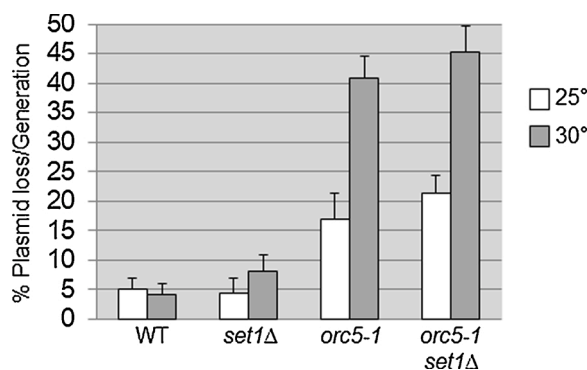


Fig. 2. Testing the *orc5-1 set1Δ* genetic interaction through an origin-dependent plasmid maintenance assay. Plasmid loss rates of an ARS-CEN-bearing plasmid (pRM102) were measured in wild-type, *set1Δ*, *orc5-1* and *orc5-1 set1Δ* strains at the temperatures of 25° and 30°. Loss rates are reported per cell division (see Materials and Methods). The average loss rates were obtained from two (30°) or three (25°) independent transformants for each strain, and the error bars indicate standard deviations.

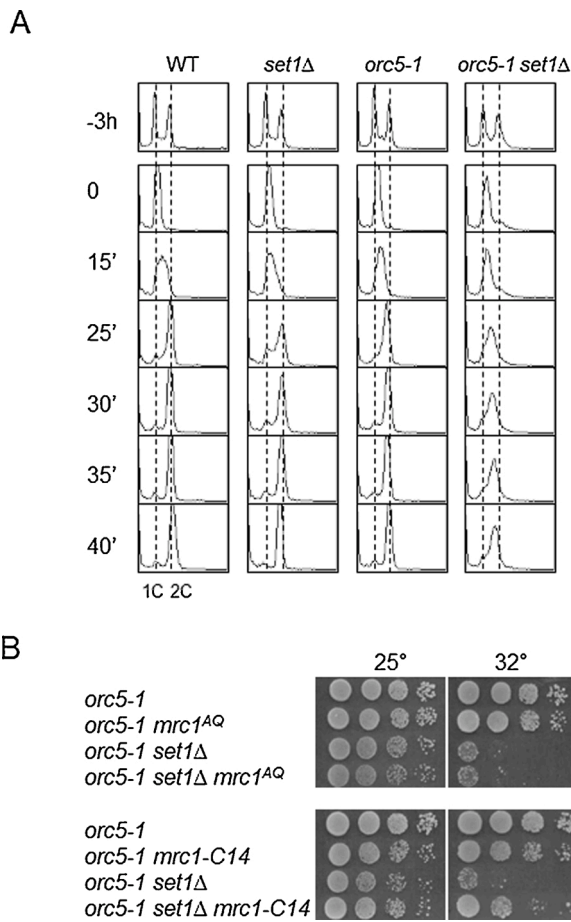


Fig. 3. The progression through S-phase is compromised in *orc5-1 set1Δ*. A) Strains grown at 25° were treated with α -factor during two hours followed by one hour at 37° before their release from the G1 block into fresh medium at 37°. DNA content was determined before (time -3 h) and after synchronization (time 0), then at the indicated intervals (minutes). B) Tenfold serial dilutions of the respective strains were spotted onto YPD plates and incubated at the indicated temperatures for 2 or 3 days.

non permissive temperature [32]. To determine whether the lack of Set1 would influence this tendency, the cell cycle profiles of non-synchronized *orc5-1* and *orc5-1 set1Δ* cultures were monitored for extended period of time after shift from 25° to 37° (Fig. S2B). We found that unlike *orc5-1*, most of the *orc5-1 set1Δ* cells accumulated in S-phase. In agreement with the results obtained with synchronized cultures (Fig. 3A), it appears that the progression through S-phase becomes the main limiting step in *orc5-1 set1Δ* at 37°.

We tested whether the *orc5-1 set1Δ* genetic interaction extends to DNA replication that occurs during meiosis, i.e. in the conditions for which a clear impact of *set1Δ* has been described [18]. After successive backcrosses, the *orc5-1* mutation was introgressed into the SK1 background, which allows rapid and synchronous sporulation. Suitable diploids were further obtained. As a first indication of the genetic interaction between *orc5-1* and *set1Δ*, at 25° the sporulation levels of the *orc5-1 set1Δ* diploid was severely reduced compared to that of each single mutant (Fig. S3A). After shifting G1-synchronized cells from 25° to 30°, the meiotic replication of SK1 diploids were compared (Fig. S3B). As already published [18], the meiotic replication in *set1Δ* cells is delayed. In *orc5-1 set1Δ* cells, the decrease of the 2C peak, which reflects the entry into S-phase, was not accompanied by a parallel increase of the 4C peak and most of the cells appear eventually blocked throughout S-phase. This correlates with the fact that only a fraction of *orc5-1 set1Δ* cells complete meiosis up to the stage of spore formation (Fig. S3A).

Thus, as in vegetative conditions, the progression through S-phase in meiotic cells appears to be strongly affected when *set1Δ* is combined with the *orc5-1* mutation.

Finally, we compared the effect of two separation-of-function mutations of the S-phase checkpoint protein Mrc1: the *mrc1-AQ* allele that fails to activate Rad53 in response to replicative stress [33] and the *mrc1-C14* allele that is checkpoint-proficient but exhibits a delayed and extended S phase progression similar to *mrc1Δ* [34]. We found that contrary to *mrc1-AQ*, the *mrc1-C14* mutation significantly improves the survival of *orc5-1 set1Δ*. Because the *mrc1-C14* mutation specifically reduces fork progression rate [35], it suggests that the negative genetic interaction between *orc5-1* and *set1Δ* is related to abnormal fork kinetics (see below).

3.4. Differential sensitivity of *orc5-1* and *orc5-1 set1Δ* to checkpoint inhibition

The involvement of the spindle assembly checkpoint (SAC) in response to defects in ORC function has been revealed by the mitigation of *orc1-161* associated cell lethality by the deletion of *MAD2* [36]. Similarly, we found that *mad2Δ* increased the viability of *orc5-1* at the non-permissive temperature of 35° (Figs. 4A and S4A for independent clones), suggesting that SAC activation restrains the growth of *orc5-1*. Although the way SAC is activated when ORC function is compromised is unclear, this could be linked to the contribution of ORC function to sister chromatid cohesion [37,38]. Such a rescue is not seen when the mitotic exit network regulator Bub2 is absent or in the presence of *rad53K227A*, a kinase deficient allele of *RAD53* (Figs. 4A and S4A). The fact that the *rad53-K227A* mutation aggravates the thermosensitivity of *orc5-1* even when Mad2 is missing could indicate that the functionality and/or structure of replication forks are compromised (see discussion). We further observed that the loss of Mad2 does not rescue the thermosensitivity of *orc5-1 set1Δ* at 35°, although a positive effect can be observed at the lower temperature of 34° (Fig. S4B). This suggests that above a certain temperature, i.e. some degree of Orc5 inactivation, an additional Mad2-independent checkpoint is activated, which restrains proliferation in *orc5-1 set1Δ* even in the absence of SAC activity.

This difference regarding the effect of Mad2 loss is reflected in the cell cycle profiles from liquid cultures, after shifting the cells to the same temperature of 35° (Fig. 4B). In *orc5-1*, the absence of Mad2 has no impact on the short-term accumulation of cells with a 2C DNA content (8 h) but is then followed by a normal cell cycle profile (24 h) which is consistent with the rescue of colony growth observed on solid medium (Fig. 4A). Such a return to a normal cell cycle is not observed for *orc5-1 set1Δ mad2Δ*, with a 24 h cell cycle profile being similar to that of *orc5-1*, again in agreement with the absence of colony growth on solid medium. The transient G2/M accumulation observed when Mad2 is missing suggests that another pathway could limit the metaphase-to-anaphase transition. The critical target of the Mad2-dependent spindle checkpoint, the inhibitor of anaphase Pds1, is also targeted by the DNA damage checkpoint kinase Chk1 [39]. Although with a limited effect on its own, the loss of Chk1 when Mad2 is absent strongly reduced the short-term G2/M accumulation (8 h) and restored a normal cell cycle distribution in *orc5-1 set1Δ* after 24 h (Fig. 4B). Thus, whereas a defective Orc5 leads to SAC activation, the additional loss of Set1 appears to be associated with the activation of a DNA damage checkpoint that restrains *orc5-1 set1Δ* cell cycle progression in the absence of Mad2.

The major DNA damage checkpoint kinase Mec1 has been proposed to act upstream of both Mad2 and Chk1 in the control of the G2/M to anaphase transition [40]. According to this model, the inactivation of Mec1 would have the same effect as the simultaneous inactivation of Mad2 and Chk1. The essential role in cell viability of Mec1 can be bypassed by deletion of *SML1* which increases dNTP levels [41]. Although Sml1 inactivation has no positive effect on its own, excluding a role for limiting amounts of dNTPs, inactivation of Mec1 alleviated the cell multiplication restriction of *orc5-1* and *orc5-1 set1Δ* at 35° (Fig. 4C,

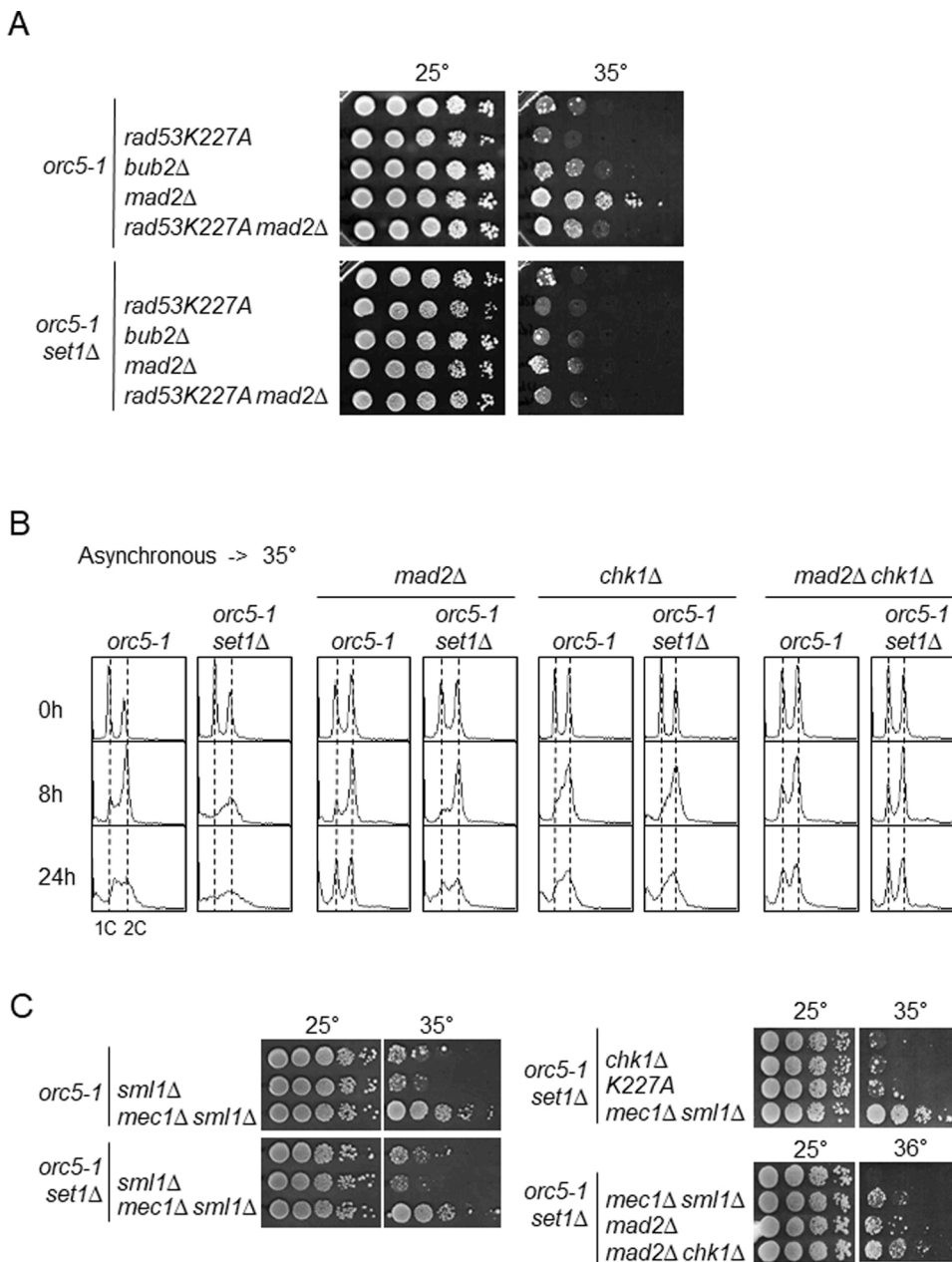


Fig. 4. Contribution of the spindle assembly checkpoint and the DNA damage checkpoint to cell cycle arrest in *orc5-1* and *orc5-1 set1Δ*. A) Different impact of *mad2Δ* on the thermosensitivity of *orc5-1* and *orc5-1 set1Δ*. Tenfold serial dilutions of the respective strains were spotted onto YPD plates and incubated at the indicated temperatures for 3 (25°) or 4 (35°) days. B) Unsynchronized cultures (25°) of the indicated strains were shifted to 35°. DNA content was determined at the indicated times (hours). 1C and 2C (broken lines) indicate the DNA content of cells with unreplicated or fully replicated DNA, respectively. C) Rescue of *orc5-1 set1Δ* thermosensitivity by *mec1Δ*. Tenfold serial dilutions of the respective strains were spotted onto YPD plates and incubated at the indicated temperatures for 3 or 4 days.

left). Neither *rad53K227A* nor *chk1Δ* are able to rescue *orc5-1 set1Δ* under similar conditions while *mec1Δ* suppression is similar to that of *mad2Δ*, with only a limited additive effect of *chk1Δ* (Fig. 4C, right). This supports the view that the Mec1-Chk1 pathway that limits the proliferation of *orc5-1 set1Δ* cells operates primarily through the activation of Mad2.

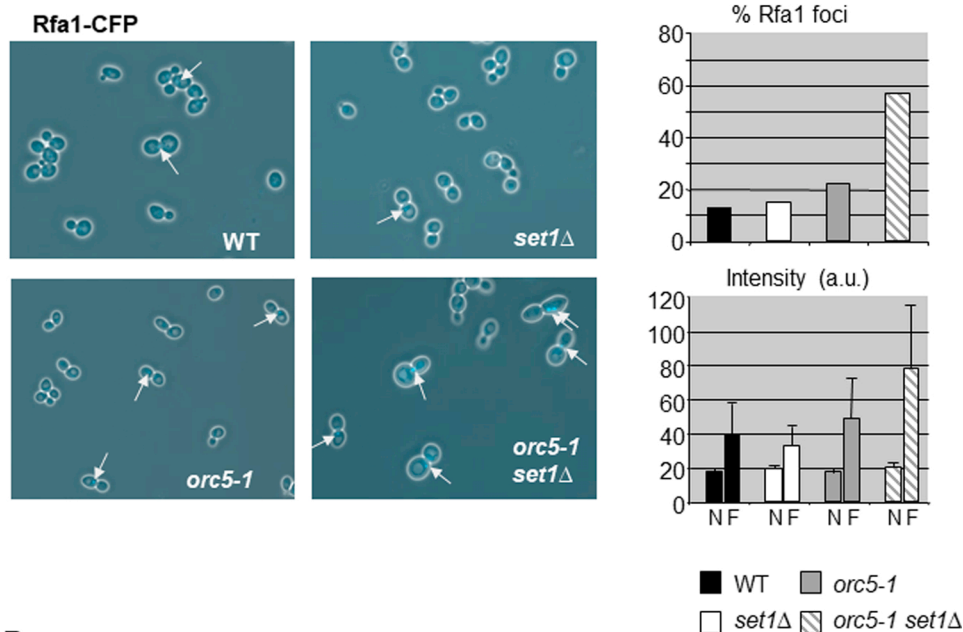
3.5. The replication stress in *orc5-1 set1Δ* is associated to a specific increase of DNA damage

According to the results described above, the absence of Set1, when associated to *orc5-1*, should lead to a measurable increase of the signal that enables activation of the Mec1-Chk1 pathway, i.e. of the RPA-coated ssDNA. To address this issue, we analyzed foci of CFP fused to Rfa1, the largest subunit of RPA, as a readout of the amount of ssDNA present in the nucleus. The percentage of cells with Rfa1 foci was measured in log phase cells at 30°, a temperature permissive for *orc5-1*, to discern more easily the specific contribution of the Set1 loss on the

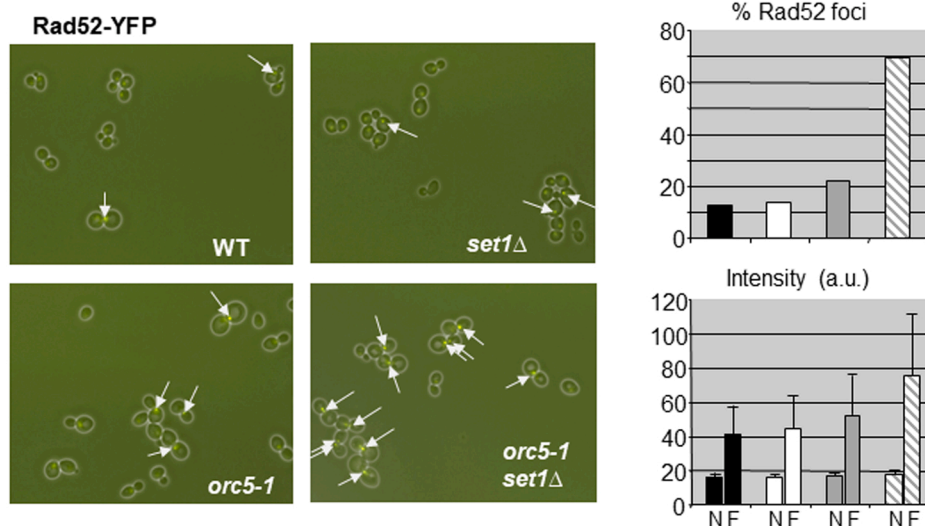
amount of ssDNA detected in the *orc5-1 set1Δ*. At this temperature, only *orc5-1 set1Δ* contains a significant fraction of G2/M arrested cells (Fig. S5). Spontaneous Rfa1 foci were found in about 13% of WT cells, the majority of which are observed during and after the S-phase, with some rare G2/M arrested cells displaying the most intense foci (Fig. 5A and data not shown). While the percentage of cells with Rfa1 foci as well as the average focus intensity were similar in *set1Δ* and only slightly higher in *orc5-1* both were significantly increased in *orc5-1 set1Δ* (Figs. 5A and S5), with a larger fraction of cells harboring more than one focus (see double arrow on microscopy photograph, Fig. 5A). The increase of brightest foci in *orc5-1 set1Δ* correlated well with that of G2/M arrested cells (Fig. S5) Thus, the impairment of S-phase progression as well as the DNA damage checkpoint activation in *orc5-1 set1Δ* is correlated to an excess of Rfa1 foci.

Some RPA-coated ssDNA may correspond to resection products of DNA double-strand breaks (DSBs) associated to stalled fork processing, whose repair depends on the Rad52-dependent homologous recombination pathway [42]. Thus, we analyzed the presence of Rad52-repair

A



B



centers by measuring Rad52 nuclear foci using a functional Rad52-YFP fusion protein. The results were very similar to those obtained with Rfa1, with more numerous and more intense Rad52 foci in *orc5-1 set1* Δ (Figs. 5B and S5). As for Rfa1, the vast majority of the most intense Rad52 foci were present in *orc5-1 set1* Δ nuclei in agreement with the larger proportion of G2/M cells (Fig. S5). As a consequence, the survival of *orc5-1 set1* Δ cells must be particularly dependent on the Rad52-dependent DNA repair activity. We confirmed this by testing the impact of Rad52 loss on cell viability and proliferation (Fig. 6). Although *orc5-1* was slightly more sensitive than the wild-type and *set1* Δ to the deletion of *RAD52* (Fig. S6), in agreement with a small increase in Rad52 foci (Fig. 5B), the lack of Rad52 was clearly most deleterious in *orc5-1 set1* Δ . Thus, most *orc5-1 set1* $\Delta rad52$ Δ spores did not give a colony at 30° (Fig. 6A) and when they did the rate of colony growth was severely affected at 25° (Fig. S6). Analysis of the DNA content of *orc5-1 set1* $\Delta rad52$ Δ at 30° shows an accumulation of cells with less than 1C DNA content, likely corresponding to dead cells (Fig. 6B).

The large increase of Rad52-dependent DNA repair activity

Fig. 5. Elevated spontaneous DNA damage levels in *orc5-1 set1* Δ cells. A) Left, microscopy photographs (merged CFP and differential interference contrast images) of cells expressing Rfa1-CFP. Arrows indicate foci. Top right, proportion (%) of cells containing Rfa1-CFP foci in exponentially growing cells (30°) of the indicated genotypes. Bottom right, average intensity (arbitrary units) of the Rfa1 foci (F) compared to the average nuclear background fluorescence (N). Error bars indicate standard deviations. B) Left, microscopy photographs (merged YFP and differential interference contrast images) of cells expressing Rad52-YFP. Arrows indicate foci. Top right, proportion (%) of cells containing Rad52-YFP foci in exponentially growing cells (30°) of the indicated genotypes. Bottom right, average intensity (arbitrary units) of the Rad52 foci (F) compared to the average nuclear background fluorescence (N). Error bars indicate standard deviations.

associated with a slow progression though S-phase unveils the replication stress that exists in *orc5-1 set1* Δ . Accordingly, one can expect a hypersensitivity of *orc5-1 set1* Δ cells to any form of additional stress that affect DNA replication. In fact, the viability of *orc5-1 set1* Δ was severely affected in the presence of hydroxyurea (HU), at concentrations sparing the viability of each single mutant (Fig. S7). Osmostress is an alternative way to impede replication fork progression [43]. Similarly, the viability of *orc5-1 set1* Δ was specifically affected when exposed to high osmolarity (Fig. S7).

3.6. Transcription replication conflicts as a source of DNA damage in *orc5-1 set1* Δ

As RNase H is able to process co-transcriptional R-loops responsible for TRCs [44], and Set1-dependent H3K4 methylation is involved in TRCs mitigation [22], we examined the effect of eliminating both RNase H1 (*rnh1* Δ) and RNase H2 (*rnh201* Δ) activities. The *orc5-1* cell viability at 31° is affected by the deletion of *RNH1* and *RNH201* (Fig. 7). One

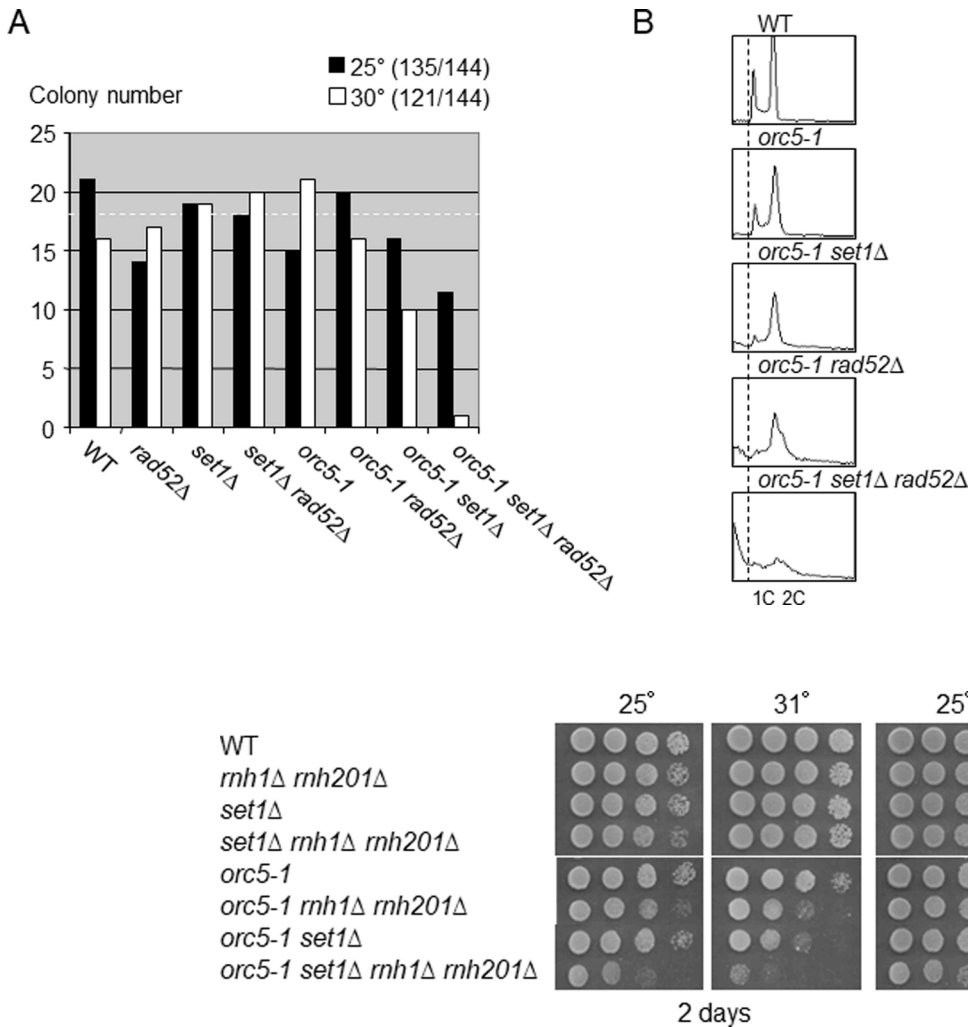


Fig. 7. Loss of Set1 sensitizes cells to RNase H removal. Tenfold serial dilutions of the respective strains were spotted onto YPD plates and incubated at the indicated temperatures for 2 and 3 days.

interpretation is that the alteration of S-phase dynamics due to *orc5-1* makes them more prone to encounter R-loops stabilized by RNase H inactivation. The negative effects of *rnh1Δ rnh201Δ* are clearly stronger when Set1 is missing as shown by the greater sensitivity of *orc5-1 set1Δ* to the lack of RNase H activity. These results argue in favor of co-transcriptional R-loops as a source of DNA damage in *orc5-1 set1Δ*, through a substantial rise of TRCs severity, as evidenced by the increase of Rad52 nuclear foci (Fig. 5B).

3.7. Limiting histone supply improves the viability of *orc5-1 set1Δ*

A reduction in histone gene dosage, which significantly lowers free histone pools, enhances survival in presence of various DNA damaging agents [45]. In line with this result, we found that deletion of *HHT2-HHF2*, one of the histone gene pairs encoding histone H3 and H4, completely suppressed the viability loss of *orc5-1 set1Δ* at 32° (Fig. 8A). We also observed that *hht2-hhf2Δ* reduced the sensitivity to HU (50 mM) of *orc5-1* and *orc5-1 set1Δ* cells (Fig. 8B). Similar results were obtained by deleting *HHT1-HHF1*, the other histone gene pair (Fig. S8). As we hypothesized that the function of H3K4 methylation could become critical in *orc5-1* cells because of the compensatory increase of replication fork rate in *orc5-1* [31], an interpretation of these results is that reduced levels of H3/H4 limit the accumulation of replication-associated DNA damage in *orc5-1 set1Δ* by decreasing replication fork velocity (see discussion).

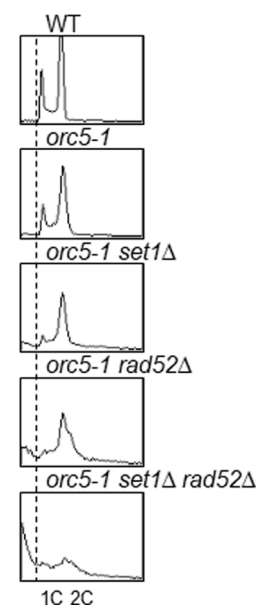


Fig. 8. Viability of *orc5-1 set1Δ* cells depends on Rad52. A) Numbers of spore colonies obtained for each genotype at 25° and 30° after tetrad dissection of the diploid strain *set1Δ/SET1 orc5-1/ORC5 rad52Δ/RAD52*. Brackets: total number of viable colonies / total number of isolated spores. The horizontal white broken line indicates the theoretical number of colonies (18 = 144 spores / 8 genotypes) expected for an even distribution of each genotype if all spores were viable. B) Cells of the indicated genotype were cultured for 5 h at 30° before their DNA content was analyzed by FACS. The fraction of cells with less than 1C DNA content (presumably dead cells) is delimited by a vertical broken line.

3.8. Oxidative stress contributes to *orc5-1 set1Δ* lethality

Whereas DNA damage accumulation is most certainly responsible for the Mec1-dependent cell cycle arrest in *orc5-1 set1Δ*, whether it contributes directly to cell death is unknown. The elevation of reactive oxygen species (ROS) levels in *orc5-1* at the non-permissive temperature of 37° [46] and the fact that Set1 loss leads to ROS accumulation during aging [47], led us to consider the oxidative stress as a cause of lethality of *orc5-1 set1Δ*. Whereas intracellular ROS levels in the single mutants were similar to that in the wild type (at 25° and 32°), a clear increase was seen for *orc5-1 set1Δ* (Fig. 9A). Differences in cell cycle profiles are not responsible for this increase (not shown) which remains after accounting for the larger cell size in *orc5-1 set1Δ* (Fig. S9A). This increase correlated with the decrease in cell viability that was specifically observed for the double mutant at 32° (Figs. 1C and 9B, top). The cell viability of *orc5-1 set1Δ* was improved in the presence of the antioxidant N-Acetylcysteine (NAC) (Fig. 9B, top), whereas it was further aggravated by the ROS hydrogen peroxide (H₂O₂) (Fig. 9B, middle). This indicates that ROS are, at least partly, responsible for the cell lethality of *orc5-1 set1Δ*. Such a causal link was reinforced by the mitigating effect the loss of the ROS responsive metacaspase Yca1 had on the *orc5-1 set1Δ* thermosensitivity (Fig. 9B, bottom).

Differences in mitochondrial respiratory activity, the main source of intracellular ROS, could be responsible for the observed differences in ROS levels. To test this, we altered mitochondrial respiratory activity in

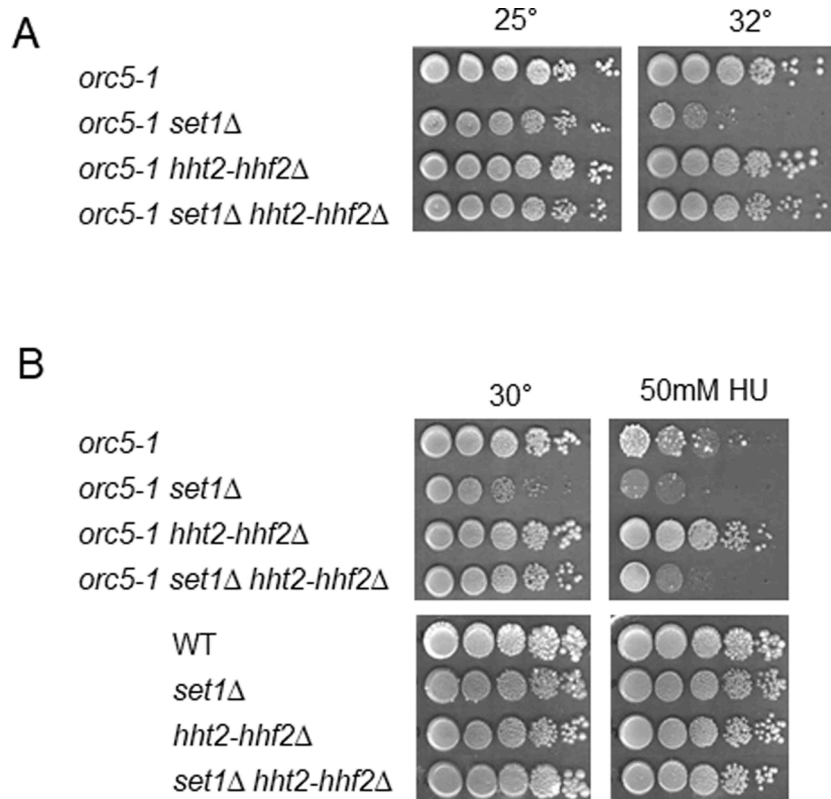


Fig. 8. Reduction in histone gene dosage limits the negative effect of Set1 loss and hydroxyurea on *orc5-1*. A) and B) Tenfold serial dilutions of the respective strains were spotted onto YPD plates without or with HU (50 mM) and incubated at the indicated temperatures for 3-4 days.

two ways (Fig. S9B). First, by using glycerol, a non-fermentable carbon source, in place of glucose, to strongly stimulate respiration. Second, by generating cells lacking mtDNA that are respiration-deficient (ρ^0). In each case, the viability of *orc5-1 set1Δ* cells remains specifically affected at 32°, showing that it is independent of the respiratory activity of mitochondria.

As both DNA damage and ROS levels are increased in *orc5-1 set1Δ*, the question arises whether a relationship exists between the two, with either ROS inducing DNA damage or the other way around. To get insight into this question, we tested whether ROS mitigation by NAC had an effect on the perturbed cell cycle distribution displayed by *orc5-1 set1Δ* at 32° (Fig. 9C). For this purpose, *orc5-1 set1Δ* cells were grown at 25° and 32° in either presence or absence of NAC. At 25°, the addition of NAC had some discernible influence on the cell cycle profile, with an increase of the G1 to G2/M ratio. At 32°, the relative accumulation of cells along the S-phase was insensitive to the presence of NAC, despite the clear mitigation of ROS levels. This suggests that the increase of ROS levels is not a cause of the defective S-phase progression in *orc5-1 set1Δ*. Similarly, it has been shown that the DNA damage observed in *orc2-1* cells at high temperature is produced independently of ROS [46]. Therefore, we propose that the DNA damage is responsible for elevated ROS production [48] in the *orc5-1 set1Δ* mutant, and this increase in ROS in its turn accounts, at least in part, for the double mutant lethality.

4. Discussion

Our conclusion that the genetic interaction between *orc5-1* and *set1Δ* results from defects in replication fork progression is primarily based on the marked S-phase lengthening manifested in *orc5-1 set1Δ* (Fig. 3) associated to DNA damage accumulation (Figs. 5 and S5). As the proximal consequence of the *orc5-1* mutation is a weakening of origin activity, the problematic replication fork progression in *orc5-1 set1Δ* could be the consequence of an additional decrease in origin firing. This would

fit with the requirement of H3K4 methylation for the full function of the *ARS1* origin, appreciated through a plasmid stability assay [11]. However, this appears not generalizable as no global origin firing deficiency has been observed in *set1Δ* [21] and recruitment/activation of replication initiation factors on various chromosomal origins appeared normal when H3K4 di-trimethylation is absent due to the loss of H2B ubiquitylation [19]. Additionally, we were unable to detect any additive effect of Set1 loss on the minichromosome maintenance defect associated with *orc5-1* (Fig. 2). Although a plasmid loss phenotype can result from various types of replication and segregation defects, this strongly suggests that a synthetic reduction in origin activity is not sufficient to explain the *orc5-1 set1Δ* genetic interaction.

The question arises about how the *orc5-1* mutation renders the S-phase sensitive to Set1 loss. Several evidences point to the intimate connection between the speed of replication forks and the frequency of origin activation. Altering replication fork speed trigger secondary responses in origins [49,50], and, conversely, decreasing the number of active origins induce compensatory increase in fork speed, partly due to higher dNTP availability [31,51]. Such compensatory increase in the rate of fork progression in *orc5-1* could explain our inability to detect a defect in S-phase progression through DNA content analysis. The premise that a faster replication fork progression is involved in the *orc5-1 set1Δ* genetic interaction is also supported by (i) the rescuing effect of lowering histone dosage that is known to limit fork speed [52], (ii) the negative effect of Sml1 loss on *orc5-1 set1Δ* viability (Fig. 5C) given that an increase in the pool of dNTPs accelerates fork progression [51], and (iii) the recent identification of a negative control that H3K4 methylation exerts on fork velocity [22]. Additionally, the negative control that Rad53 exerts on the rate of fork progression under replication stress conditions [53] could explain the sensitivity of *orc5-1* to Rad53 inactivation (Figs. 4A and S4A).

One can expect that mutations that affect proteins involved in replication fork progression in addition to origin use, such as Cdc17,

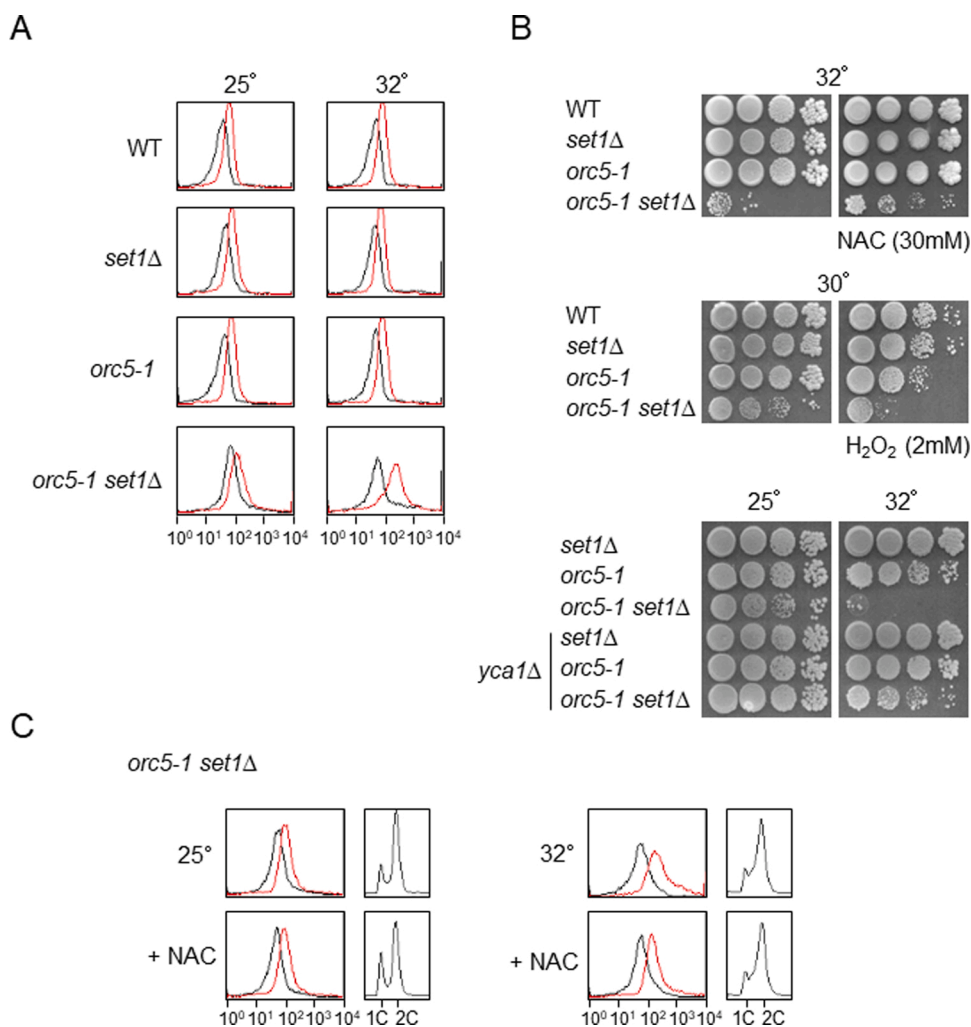


Fig. 9. Oxidative stress is involved in *orc5-1 set1Δ* lethality. A) The indicated strains were cultured at either 25° or 32° before ROS levels were determined at 7 h. The fluorescence signals measured in absence (black) or presence (red) of the ROS-sensitive fluorochrome (CellROX green) are superimposed. X-axis and y-axis: fluorescence intensity (log scale) and number of cells, respectively. B) The viability of *orc5-1 set1Δ* is sensitive to NAC, H₂O₂ and *yca1Δ*. Tenfold serial dilutions of the respective strains were spotted onto YPD plates at the indicated temperatures for 3-4 days. NAC and H₂O₂ concentrations are indicated. C) Decreasing ROS levels is without effect on the S-phase progression defect in *orc5-1 set1Δ*. Cells were cultured at 25° and 32°, in absence or presence of NAC (30 mM), before ROS levels (left) and DNA content (right) were determined at 7 h.

Cdc7 and Cdc45, display weaker or no synthetic growth defects when combined with *set1Δ*. In fact, this is clearly not the case (see Fig. S1 for Cdc17, [11] for Cdc7 and Cdc45). However, since in fact replication forks proceed more rapidly in cells depleted for Cdc7 [31], an increase in replication fork speed could be involved in each case. Similarly, the negative impact of HU on the double mutant viability merits an explanation. This might seem unexpected since the primary effect of HU, the decrease of the dNTP pool (through RNR inhibition), could have improved the viability. However, replication forks arrested by short-term HU treatment accumulate ssDNA [54], notably through the resection of nascent DNA [21]. In contrast, ssDNA formation is not detected at replication sites in cells with inhibited biosynthesis of the histones [52]. This difference in ssDNA accumulation could explain why, despite both slowing down replication fork velocity, reducing the dNTP pool and depleting histone have opposite effect on *orc5-1 set1Δ* viability. Additionally, the fact that oxidative stress may contribute to the cytotoxic effect of HU [55] must be taken into account given the involvement of ROS in *orc5-1 set1Δ* lethality (Fig. 9).

The local reduction of RPA-bound ssDNA at HU-stalled forks in *set1Δ* [21] seemingly contradicts the global increase of ssDNA observed in the *orc5-1 set1Δ*, estimated through the analysis of nuclear Rfa1 foci. Assuming that, as proposed [21], the loss of Set1 also effectively limits the nucleolytic degradation of nascent DNA in *orc5-1 set1Δ*, one simple explanation is that the restricted production of ssDNA at individual stalled fork is largely surpassed by an increase in the number of stalled forks. Alternatively, the forks whose progression is impaired in *orc5-1 set1Δ* may be not equivalent to HU-stalled forks and are not processed in

the same way.

Meiotic DNA replication appears to be more sensitive to the combination of *orc5-1* and *set1Δ* mutations than mitotic cells at a temperature fully permissive for *orc5-1* (Fig. S3B). Some characteristics of the meiotic S-phase can explain this increased sensitivity such as the fact that replication origins are on average less frequently activated [56], and that the amount of dNTPs is more limited [57]. Thus, meiotic S-phase can be considered to occur in mild replication stress conditions that would be equivalent to the presence of limited amounts of HU in mitotic cells. This illustrates how the physiological context can influence the degree to which replication fork progression is sensitive to the lack of Set1-dependent H3K4 methylation.

Considering the results of our study in the context of published work, we propose the following model for the *orc5-1 set1Δ* genetic interaction (Fig. 10). Two consequences of the *orc5-1* mutation can be considered (Fig. 10, middle panel). On one hand, as described previously [36], the activation of a Mad2-dependent pathway, possibly the SAC, seems primary responsible for the G2/M arrest that restrict cell division when ORC is defective, whereas a reduction in the number of functional replication forks compromises the activation of the DNA damage checkpoint during S-phase [58]. The checkpoint initiating signal can be a defect in kinetochore-spindle attachment and/or in sister chromatid cohesion [37,38]. On the other hand, the weaker level of origin firing caused by *orc5-1* results in an increase of the replication fork speed [31]. This increase can potentially induce some replication stress [59], in particular at highly transcribed regions because of TRCs. The slowing down of the replicon by Set1-dependent H3K4 methylation, as it passes

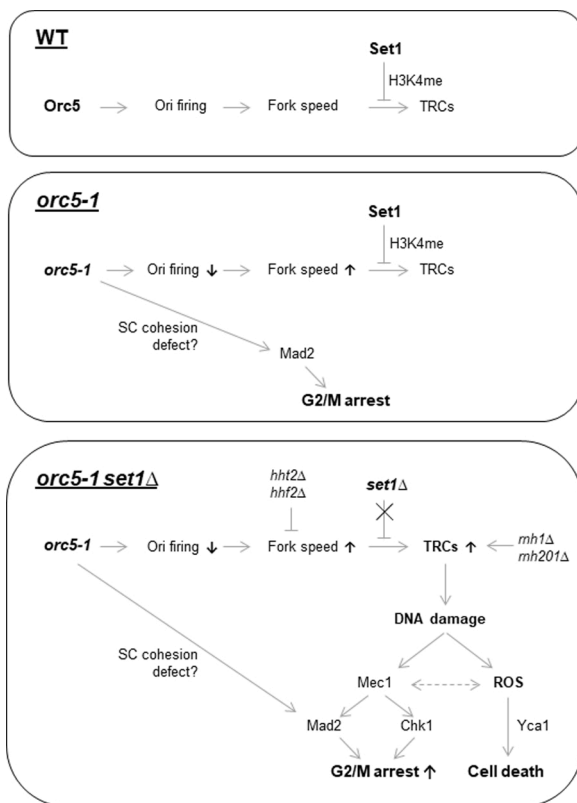


Fig. 10. Proposed model for the genetic interaction between *orc5-1* and *set1Δ*. In the wild type (top), Orc5 ensures proper origin firing and Set1, through the transcription-deposited H3K4 methylation, helps to avoid the occurrence of TRCs at highly transcribed regions. The *orc5-1* mutation has two consequences (middle): first, the activation of Mad2 (via sister chromatid cohesion defect?) that lead to a G2/M arrest, and second, an increase of replication fork speed that compensates for weaker levels of origin firing. The increase in fork velocity is efficiently dampened by Set1-dependent H3K4 methylation, relieving highly transcribed regions from TRCs. In absence of Set1 (bottom), unrestrained fork progression at highly transcribed regions elevates the frequency of TRCs which are even more frequent if co-transcriptional R-loops are stabilized when RNase H activity is missing (*rnh1Δ rnh201Δ*). Conversely, lowering the histone levels (*hht2Δ hhf2Δ*) counteracts the fork rate increase due to *orc5-1* mutation, and thus relieves TRCs in absence of Set1. The DNA damage associated to TRCs reinforces the G2/M arrest, through activation of the Mec1-Chk1 signaling, and can induce a Yca1-dependent cell death, as a consequence of ROS production. See discussion for details.

through highly expressed ORFs, turns out to be important to protect the genome from TRCs [22]. Accordingly, in the absence of Set1 (Fig. 10, bottom panel), unrestrained fork progression caused by the reduction in origin firing in *orc5-1*, could lead to frequent TRCs, resulting in R-loops formation that will stall replication forks and thus impede S-phase progression. TRCs are promoted by the removal of RNase H activity (*rnh1-rnh201Δ*) which stabilizes co-transcriptional R-loops. In contrary, lowering of the histone levels (*hht2-hhf2Δ*) would limit the occurrence of TRCs in absence of Set1 by counteracting the fork rate increase due to *orc5-1* mutation. The effect of reduced histone dosage on fork speed could be indirect, through an increase of origin firing frequency, by facilitating ORC binding and pre-RC assembly, or direct due to the functional coupling between replication fork progression and nucleosome assembly [52]. Why HU causes synthetic sickness in *orc5-1 set1Δ* while reducing the rate of forks is unclear. Some features of HU-slowed forks, such as decoupling between polymerases and helicases, is a possible reason.

R-loops are responsible for stalled forks at TRCs sites, and both are associated with ssDNA bound by RPA [4,10]. Nucleolytic processing of

the ssDNA can generate DSBs, the resection of which can generate additional ssDNA required for their Rad52-dependent repair. Whatever its origin, the RPA-covered ssDNA is responsible for the excess of Rfa1 foci in *orc5-1 set1Δ* and activates Mec1 which, through both Mad2 and Chk1, reinforces the G2/M arrest of the *orc5-1* mutant (Fig. 10, bottom panel). DNA damages, in the form of ssDNA and DSBs, are also a source of ROS [48]. Our data indicates that, above a certain threshold, ROS can induce a Yca1-dependent cell death. These two consequences of DNA damage - cell cycle arrest and ROS production - may be not independent as a mutual feed-forward relationship exists between Mec1 and ROS, with ROS production being partly dependent on Mec1 [46] and Mec1 activity requiring some ROS [60].

The role for Set1 in TRCs prevention was proposed in the specific context of checkpoint-defective (*rad53* mutants) cells treated with HU [22]. In this context, the fact that H3K4 methylation favors forks stalling at highly transcribed regions compromises their integrity, and the relief of this impediment to fork progression by ablating Set1 improves cell viability. Such a positive outcome contrasts with the negative impact of Set1 loss on cell viability when associated with the *orc5-1* mutation. This shows that the effect of Set1 ablation is context sensitive and can have opposite outcomes according to the way replication stress is induced. In checkpoint defective cells (*rad53* mutants) during an HU-induced stress, the structure and functionality of stalled forks is not preserved and relieving the impediment to fork progression due to H3K4 methylation is overall beneficial [22]. In checkpoint proficient cells (our study), the increase of fork velocity due to *orc5-1* favors the occurrence of TRCs and removing the protection provided by H3K4 methylation becomes detrimental. Our finding thus strengthens the notion that one major role of H3K4 methylation is to preserve the integrity of replication forks by modulating their velocity at the level of highly transcribed regions.

Author contribution statement

Christophe de La Roche Saint-André: Conceptualization, Methodology, Data curation, Writing-Original draft preparation.

Vincent Géli: Funding acquisition, Writing-Reviewing and Editing.

Declaration of Competing Interest

The authors report no declarations of interest.

Acknowledgements

We thank Valérie Garcia, Christelle Cayrou and Dmitri Churikov for critical reading of the manuscript; Morgane Joessel and Gaëtan Vaccari for their contribution in this work during their training course in the laboratory; Michael Weinreich for the *orc5-1*, *cdc6-4*, *mcm2-1* and *cdc17-1* strains; Philippe Pasero and Stephen Elledge for the *mrc1^{AQ}* strain and the *mrc1-C14* strain, respectively; Akash Gunjan for strains harboring the *hht1-hhf1Δ* and *hht2-hhf2Δ* loci; Nicanor Austriaco for the strain harboring the *yca1Δ* locus. This work was supported by the Ligue Nationale Contre le Cancer (Equipe labellisée, LNCC-EL-2020) and by the Agence Nationale de la Recherche (ANR-19-CE12-0023 NIRO). The funders had no role in study design, data collection and analysis, decision to publish, or preparation of the manuscript.

Appendix A. Supplementary data

Supplementary material related to this article can be found, in the online version, at doi:<https://doi.org/10.1016/j.dnarep.2021.103159>.

References

- [1] S.P. Bell, K. Labib, Chromosome duplication in *Saccharomyces cerevisiae*, *Genetics* 203 (2016) 1027–1067, <https://doi.org/10.1534/genetics.115.186452>.

- [2] B. Gómez-González, A. Aguilera, Transcription-mediated replication hindrance: a major driver of genome instability, *Genes Dev.* 33 (2019) 1008–1026, <https://doi.org/10.1101/gad.324517.119>.
- [3] S. Hamperl, M.J. Bocek, J.C. Saldívar, T. Swigut, K.A. Cimprich, Transcription-replication conflict orientation modulates R-Loop levels and activates distinct DNA damage responses, *Cell* 170 (2017) 774–786.e19, <https://doi.org/10.1016/j.cell.2017.07.043>.
- [4] H.D. Nguyen, T. Yadav, S. Giri, B. Saez, T.A. Graubert, L. Zou, Functions of replication protein A as a sensor of R loops and a regulator of RNaseH1, *Mol. Cell* 65 (2017) 832–847.e4, <https://doi.org/10.1016/j.molcel.2017.01.029>.
- [5] S.A. Sabatino, S.L. Forsburg, Managing single-stranded DNA during replication stress in fission yeast, *Biomolecules* 5 (2015) 2123–2139, <https://doi.org/10.3390/biom5032123>.
- [6] L. Zou, S.J. Elledge, Sensing DNA damage through ATRIP recognition of RPA-ssDNA complexes, *Science* 300 (2003) 1542–1548, <https://doi.org/10.1126/science.1083430>.
- [7] D. Shechter, V. Costanzo, J. Gautier, Regulation of DNA replication by ATR: signaling in response to DNA intermediates, *DNA Repair (Amst)* 3 (2004) 901–908, <https://doi.org/10.1016/j.dnarep.2004.03.020>.
- [8] T.A. Weinert, G.L. Kiser, L.H. Hartwell, Mitotic checkpoint genes in budding yeast and the dependence of mitosis on DNA replication and repair, *Genes Dev.* 8 (1994) 652–665, <https://doi.org/10.1101/gad.8.6.652>.
- [9] M. Moriel-Carretero, A. Aguilera, A postincision-deficient TFIIF causes replication fork breakage and uncovers alternative Rad51- or Pol32-mediated restart mechanisms, *Mol. Cell* 37 (2010) 690–701, <https://doi.org/10.1016/j.molcel.2010.02.008>.
- [10] C. Allen, A.K. Ashley, R. Hromas, J.A. Nickoloff, More forks on the road to replication stress recovery, *J. Mol. Cell Biol.* 3 (2011) 4–12, <https://doi.org/10.1093/jmcb/mjq049>.
- [11] L.F. Rizzardi, E.S. Dorn, B.D. Strahl, J.G. Cook, DNA replication origin function is promoted by H3K4 di-methylation in *Saccharomyces cerevisiae*, *Genetics* 192 (2012) 371–384, <https://doi.org/10.1534/genetics.112.142349>.
- [12] C. Costas, M. de la Paz Sanchez, H. Stroud, Y. Yu, J.C. Oliveros, S. Feng, et al., Genome-wide mapping of Arabidopsis thaliana origins of DNA replication and their associated epigenetic marks, *Nat. Struct. Mol. Biol.* 18 (2011) 395–400, <https://doi.org/10.1038/nsmb.1988>.
- [13] M.S. Valenzuela, Y. Chen, S. Davis, F. Yang, R.L. Walker, S. Bilke, et al., Preferential localization of human origins of DNA replication at the 5'-ends of expressed genes and at evolutionarily conserved DNA sequences, *PLoS One* 6 (2011), e17308, <https://doi.org/10.1371/journal.pone.0017308>.
- [14] B. Miotto, Z. Ji, K. Struhl, Selectivity of ORC binding sites and the relation to replication timing, fragile sites, and deletions in cancers, *Proc. Natl. Acad. Sci. U. S. A.* 113 (2016) E4810–4819, <https://doi.org/10.1073/pnas.1609060113>.
- [15] B. Rondinelli, H. Schwerer, E. Antonini, M. Gaviraghi, A. Lupi, M. Frenquelli, et al., H3K4me3 demethylation by the histone demethylase KDM5C/JARID1C promotes DNA replication origin firing, *Nucleic Acids Res.* 43 (2015) 2560–2574, <https://doi.org/10.1093/nar/gkv090>.
- [16] F. Lu, X. Wu, F. Yin, C. Chia-Fang Lee, M. Yu, L.S. Mihaylov, et al., Regulation of DNA replication and chromosomal polyploidy by the MLL-WDR5-RBBP5 methyltransferases, *Biol. Open* 5 (2016) 1449–1460, <https://doi.org/10.1242/bio.019729>.
- [17] T.H. Beilharz, P.F. Harrison, D.M. Miles, M.M. See, U.M.M. Le, M. Kalanon, et al., Coordination of cell cycle progression and mitotic spindle assembly involves histone H3 lysine 4 methylation by Set1/COMPASS, *Genetics* 205 (2017) 185–199, <https://doi.org/10.1534/genetics.116.194852>.
- [18] J. Sollier, W. Lin, C. Soustelle, K. Suhre, A. Nicolas, V. Géli, et al., Set1 is required for meiotic S-phase onset, double-strand break formation and middle gene expression, *EMBO J.* 23 (2004) 1957–1967, <https://doi.org/10.1038/sj.emboj.7600204>.
- [19] K.M. Trujillo, M.A. Osley, A role for H2B ubiquitylation in DNA replication, *Mol. Cell* 48 (2012) 734–746, <https://doi.org/10.1016/j.molcel.2012.09.019>.
- [20] Z.-W. Sun, C.D. Allis, Ubiquitination of histone H2B regulates H3 methylation and gene silencing in yeast, *Nature* 418 (2002) 104–108, <https://doi.org/10.1038/nature00883>.
- [21] A. Delamarre, A. Barthe, C. de la Roche Saint-André, P. Luciano, F. Forey, I. Padioleau, et al., MRX increases chromatin accessibility at stalled replication forks to promote nascent DNA resection and cohesin loading, *Mol. Cell* 77 (2020) 395–410.e3, <https://doi.org/10.1016/j.molcel.2019.10.029>.
- [22] S.Y. Chong, S. Cutler, J.-J. Lin, C.-H. Tsai, C.-H. Tsai, S. Biggins, et al., H3K4 methylation at active genes mitigates transcription-replication conflicts during replication stress, *Nat. Commun.* 11 (2020), 809, <https://doi.org/10.1038/s41467-020-14595-4>.
- [23] L. Acquaviva, L. Székvölgyi, B. Dichtl, B.S. Dichtl, C. de La Roche Saint André, A. Nicolas, et al., The COMPASS subunit Spp1 links histone methylation to initiation of meiotic recombination, *Science* 339 (2013) 215–218, <https://doi.org/10.1126/science.1225739>.
- [24] C.A. Schneider, W.S. Rasband, K.W. Eliceiri, NIH Image to ImageJ: 25 years of image analysis, *Nat. Methods* 9 (2012) 671–675, <https://doi.org/10.1038/nmeth.2089>.
- [25] R.K. Mann, M. Grunstein, Histone H3 N-terminal mutations allow hyperactivation of the yeast GAL1 gene in vivo, *EMBO J.* 11 (1992) 3297–3306.
- [26] C. Liang, M. Weinreich, B. Stillman, ORC and Cdc6p interact and determine the frequency of initiation of DNA replication in the genome, *Cell* 81 (1995) 667–676, [https://doi.org/10.1016/0092-8674\(95\)90528-6](https://doi.org/10.1016/0092-8674(95)90528-6).
- [27] P.-M. Dehé, B. Dichtl, D. Schaft, A. Roguev, M. Pamblanco, R. Lebrun, et al., Protein interactions within the Set1 complex and their roles in the regulation of histone 3 lysine 4 methylation, *J. Biol. Chem.* 281 (2006) 35404–35412, <https://doi.org/10.1074/jbc.M603099200>.
- [28] B. Guillemette, P. Drogaris, Lin H-HS, H. Armstrong, K. Hiragami-Hamada, A. Imhof, et al., H3 lysine 4 is acetylated at active gene promoters and is regulated by H3 lysine 4 methylation, *PLoS Genet.* 7 (2011), e1001354, <https://doi.org/10.1371/journal.pgen.1001354>.
- [29] M.C. Espinosa, M.A. Rehman, P. Chisamore-Robert, D. Jeffery, K. Yankulov, GCN5 is a positive regulator of origins of DNA replication in *Saccharomyces cerevisiae*, *PLoS One* 5 (2010) e8964, <https://doi.org/10.1371/journal.pone.0008964>.
- [30] C. Bian, C. Xu, J. Ruan, K.K. Lee, T.L. Burke, W. Tempel, et al., Sgf29 binds histone H3K4me2/3 and is required for SAGA complex recruitment and histone H3 acetylation, *EMBO J.* 30 (2011) 2829–2842, <https://doi.org/10.1038/emboj.2011.193>.
- [31] Y. Zhong, T. Nellimoottil, J.M. Peace, S.R.V. Knott, S.K. Villwock, J.M. Yee, et al., The level of origin firing inversely affects the rate of replication fork progression, *J. Cell Biol.* 201 (2013) 373–383, <https://doi.org/10.1083/jcb.201208060>.
- [32] A. Dillin, J. Rine, Roles for ORC in M phase and S phase, *Science* 279 (1998) 1733–1737, <https://doi.org/10.1126/science.279.5357.1733>.
- [33] A.J. Osborn, Mrc1 is a replication fork component whose phosphorylation in response to DNA replication stress activates Rad53, *Genes Dev.* 17 (2003) 1755–1767, <https://doi.org/10.1101/gad.1098303>.
- [34] M.L. Naylor, J.-m. Li, A.J. Osborn, S.J. Elledge, Mrc1 phosphorylation in response to DNA replication stress is required for Mec1 accumulation at the stalled fork, *Proc. Natl. Acad. Sci.* 106 (2009) 12765–12770, <https://doi.org/10.1073/pnas.0904623106>.
- [35] A. Gispan, M. Carmi, N. Barkai, Checkpoint-independent scaling of the *Saccharomyces cerevisiae* DNA replication program, *BMC Biol.* 12 (2014) 79, <https://doi.org/10.1186/s12915-014-0079-z>.
- [36] D.G. Gibson, S.P. Bell, O.M. Aparicio, Cell cycle execution point analysis of ORC function and characterization of the checkpoint response to ORC inactivation in *Saccharomyces cerevisiae*, *Genes Cells* 11 (2006) 557–573, <https://doi.org/10.1111/j.1365-2443.2006.00967.x>.
- [37] B. Suter, A. Tong, M. Chang, L. Yu, G.W. Brown, C. Boone, et al., The origin recognition complex links replication, sister chromatid cohesion and transcriptional silencing in *Saccharomyces cerevisiae*, *Genetics* 167 (2004) 579–591, <https://doi.org/10.1534/genetics.103.024851>.
- [38] K. Shimada, S.M. Gasser, The origin recognition complex functions in sister-chromatid cohesion in *Saccharomyces cerevisiae*, *Cell* 128 (2007) 85–99, <https://doi.org/10.1016/j.cell.2006.11.045>.
- [39] H. Wang, D. Liu, Y. Wang, J. Qin, S.J. Elledge, Pds1 phosphorylation in response to DNA damage is essential for its DNA damage checkpoint function, *Genes Dev.* 15 (2001) 1361–1372, <https://doi.org/10.1101/gad.893201>.
- [40] E.M. Kim, D.J. Burke, DNA damage activates the SAC in an ATM/ATR-dependent manner, independently of the kinetochore, *PLoS Genet.* 4 (2008), e1000015, <https://doi.org/10.1371/journal.pgen.1000015>.
- [41] X. Zhao, E.G. Muller, R. Rothstein, A suppressor of two essential checkpoint genes identifies a novel protein that negatively affects dNTP pools, *Mol. Cell* 2 (1998) 329–340, [https://doi.org/10.1016/s1097-2765\(00\)80277-4](https://doi.org/10.1016/s1097-2765(00)80277-4).
- [42] J.H. Petrimi, D.A. Bressan, M.S. Yao, The RAD52 epistasis group in mammalian double strand break repair, *Semin. Immunol.* 9 (1997) 181–188, <https://doi.org/10.1006/smim.1997.0067>.
- [43] A. Duch, I. Felipe-Abrio, S. Barroso, G. Yaakov, M. García-Rubio, A. Aguilera, et al., Coordinated control of replication and transcription by a SAPK protects genomic integrity, *Nature* 493 (2013) 116–119, <https://doi.org/10.1038/nature11675>.
- [44] H. Zhao, M. Zhu, O. Limbo, P. Russell, RNase H eliminates R-loops that disrupt DNA replication but is nonessential for efficient DSB repair, *EMBO Rep.* 19 (2018), <https://doi.org/10.15252/embr.201745335>.
- [45] D. Liang, S.L. Burkhart, R.K. Singh, M.-H.M. Kabbaj, A. Gunjan, Histone dosage regulates DNA damage sensitivity in a checkpoint-independent manner by the homologous recombination pathway, *Nucleic Acids Res.* 40 (2012) 9604–9620, <https://doi.org/10.1093/nar/gks722>.
- [46] M. Weinberger, L. Ramachandran, L. Feng, K. Sharma, X. Sun, M. Marchetti, et al., Apoptosis in budding yeast caused by defects in initiation of DNA replication, *J. Cell. Sci.* 118 (2005) 3543–3553, <https://doi.org/10.1242/jcs.02477>.
- [47] D. Walter, A. Matter, B. Fahrenkrog, Loss of histone H3 methylation at lysine 4 triggers apoptosis in *Saccharomyces cerevisiae*, *PLoS Genet.* 10 (2014), e1004095, <https://doi.org/10.1371/journal.pgen.1004095>.
- [48] L.A. Rowe, N. Degtyareva, P.W. Doetsch, DNA damage-induced reactive oxygen species (ROS) stress response in *Saccharomyces cerevisiae*, *Free Radic. Biol. Med.* 45 (2008) 1167–1177, <https://doi.org/10.1016/j.freeradbiomed.2008.07.018>.
- [49] X.Q. Ge, D.A. Jackson, J.J. Blow, Dormant origins licensed by excess Mcm2-7 are required for human cells to survive replicative stress, *Genes Dev.* 21 (2007) 3331–3341, <https://doi.org/10.1101/gad.457807>.
- [50] A. Ibarra, E. Schwob, J. Méndez, Excess MCM proteins protect human cells from replicative stress by licensing backup origins of replication, *Proc. Natl. Acad. Sci. U. S. A.* 105 (2008) 8956–8961, <https://doi.org/10.1073/pnas.0803978105>.
- [51] J. Poli, O. Tspanolina, L. Crabbé, A. Keszhelyi, V. Pantescio, A. Chabes, et al., dNTP pools determine fork progression and origin usage under replication stress, *EMBO J.* 31 (2012) 883–894, <https://doi.org/10.1038/emboj.2011.470>.
- [52] J. Mejlvang, Y. Feng, C. Alabert, K.J. Neelens, Z. Jasencakova, X. Zhao, et al., New histone supply regulates replication fork speed and PCNA unloading, *J. Cell Biol.* 204 (2014) 29–43, <https://doi.org/10.1083/jcb.201305017>.
- [53] J. Bacal, M. Moriel-Carretero, B. Pardo, A. Barthe, S. Sharma, A. Chabes, et al., Mrc1 and Rad9 cooperate to regulate initiation and elongation of DNA replication in response to DNA damage, *EMBO J.* 37 (2018), <https://doi.org/10.15252/emboj.201899319>.

- [54] K.A. Cimprich, D. Cortez, ATR: an essential regulator of genome integrity, *Nat. Rev. Mol. Cell Biol.* 9 (2008) 616–627, <https://doi.org/10.1038/nrm2450>.
- [55] A. Singh, Y.-J. Xu, The cell killing mechanisms of hydroxyurea, *Genes (Basel)* 7 (2016), <https://doi.org/10.3390/genes7110099>.
- [56] C. Heichinger, C.J. Penkett, J. Bähler, P. Nurse, Genome-wide characterization of fission yeast DNA replication origins, *EMBO J.* 25 (2006) 5171–5179, <https://doi.org/10.1038/sj.emboj.7601390>.
- [57] H.G. Blitzblau, C.S. Chan, A. Hochwagen, S.P. Bell, Separation of DNA replication from the assembly of break-competent meiotic chromosomes, *PLoS Genet.* 8 (2012), e1002643, <https://doi.org/10.1371/journal.pgen.1002643>.
- [58] K. Shimada, P. Pasero, S.M. Gasser, ORC and the intra-S-phase checkpoint: a threshold regulates Rad53p activation in S phase, *Genes Dev.* 16 (2002) 3236–3252, <https://doi.org/10.1101/gad.239802>.
- [59] A. Maya-Mendoza, P. Moudry, J.M. Merchut-Maya, M. Lee, R. Strauss, J. Bartek, High speed of fork progression induces DNA replication stress and genomic instability, *Nature* 559 (2018) 279–284, <https://doi.org/10.1038/s41586-018-0261-5>.
- [60] C.K. Tsang, Y. Liu, J. Thomas, Y. Zhang, X.F.S. Zheng, Superoxide dismutase 1 acts as a nuclear transcription factor to regulate oxidative stress resistance, *Nat. Commun.* 5 (2014), 3446, <https://doi.org/10.1038/ncomms4446>.